



**HAL**  
open science

# Identification of enriched hyperthermophilic microbial communities from a deep-sea hydrothermal vent chimney under electrolithoautotrophic culture conditions

Guillaume Pillot, Oulfat Amin Ali, Sylvain Davidson, Laetitia Shintu, Anne Godfroy, Yannick Combet-Blanc, Patricia Bonin, Pierre-Pol Liebgott

## ► To cite this version:

Guillaume Pillot, Oulfat Amin Ali, Sylvain Davidson, Laetitia Shintu, Anne Godfroy, et al.. Identification of enriched hyperthermophilic microbial communities from a deep-sea hydrothermal vent chimney under electrolithoautotrophic culture conditions. *Scientific Reports*, 2021, 11 (1), 10.1038/s41598-021-94135-2 . hal-03427430

**HAL Id: hal-03427430**

**<https://hal.science/hal-03427430>**

Submitted on 9 Dec 2021

**HAL** is a multi-disciplinary open access archive for the deposit and dissemination of scientific research documents, whether they are published or not. The documents may come from teaching and research institutions in France or abroad, or from public or private research centers.

L'archive ouverte pluridisciplinaire **HAL**, est destinée au dépôt et à la diffusion de documents scientifiques de niveau recherche, publiés ou non, émanant des établissements d'enseignement et de recherche français ou étrangers, des laboratoires publics ou privés.



Distributed under a Creative Commons Attribution 4.0 International License



OPEN

## Identification of enriched hyperthermophilic microbial communities from a deep-sea hydrothermal vent chimney under electrolithoautotrophic culture conditions

Guillaume Pillot<sup>1</sup>, Oulfat Amin Ali<sup>1</sup>, Sylvain Davidson<sup>1</sup>, Laetitia Shintu<sup>3</sup>, Anne Godfroy<sup>2</sup>, Yannick Combet-Blanc<sup>1</sup>, Patricia Bonin<sup>1</sup> & Pierre-Pol Liebgott<sup>1</sup>✉

Deep-sea hydrothermal vents are extreme and complex ecosystems based on a trophic chain. We are still unsure of the identities of the first colonizers of these environments and their metabolism, but they are thought to be (hyper)thermophilic autotrophs. Here we investigate whether the electric potential observed across hydrothermal chimneys could serve as an energy source for these first colonizers. Experiments were performed in a two-chamber microbial electrochemical system inoculated with deep-sea hydrothermal chimney samples, with a cathode as sole electron donor, CO<sub>2</sub> as sole carbon source, and nitrate, sulfate, or oxygen as electron acceptors. After a few days of culturing, all three experiments showed growth of electrotrophic biofilms consuming the electrons (directly or indirectly) and producing organic compounds including acetate, glycerol, and pyruvate. Within the biofilms, the only known autotroph species retrieved were members of *Archaeoglobales*. Various heterotrophic phyla also grew through trophic interactions, with *Thermococcales* growing in all three experiments as well as other bacterial groups specific to each electron acceptor. This electrotrophic metabolism as energy source driving initial microbial colonization of conductive hydrothermal chimneys is discussed.

Deep-sea hydrothermal vents are geochemical structures housing an extreme ecosystem rich in micro- and macro-organisms. Since their discovery in 1977<sup>1</sup>, they have attracted the interest of researchers and, more recently, industries with their unique characteristics. Isolated in the deep ocean, far away from sunlight and subsequent organic substrates, the primary energy sources for the development of this abundant biosphere remain elusive in these extreme, mineral-rich environments. Since their discovery, many new metabolisms have been identified based on organic or inorganic molecules. However, the driving force sustaining all biodiversity in these environments is thought to be based on chemolithoautotrophy<sup>2</sup>. Unlike most ecosystems, deep-sea ecosystems are totally dark, and microorganisms have thus adapted to base their metabolism on lithoautotrophy using inorganic compounds as the energy source to fix inorganic carbon sources.

Primary colonizers of deep-sea hydrothermal vents are assumed to be (hyper)thermophilic microbes developing near hydrothermal fluid, as retrieved in young hydrothermal chimneys. These first colonizers are affiliated to *Archaea*, such as *Archaeoglobales*, *Thermococcales*, *Methanococcales* or *Desulfurococcales*, and to *Bacteria*, for example *ε-proteobacteria* and *Aquificales*<sup>3–5</sup>. Recent studies have also shown that hyperthermophilic *Archaea*, which count among the supposed first colonizers, are able to quickly scan and fix onto surfaces to find the best conditions for growth<sup>6</sup>. These hyperthermophilic microorganisms fix inorganic carbon through

<sup>1</sup>Aix Marseille Université, Université de Toulon, IRD, CNRS, MIO UM 110, 13288 Marseille Cedex 09, France. <sup>2</sup>FREMER, CNRS, Université de Bretagne Occidentale, Laboratoire de Microbiologie des Environnements Extrêmes-UMR6197, Ifremer, Centre de Brest CS10070, Plouzané, France. <sup>3</sup>Aix Marseille Univ, CNRS, Centrale Marseille, iSm2, Marseille, France. ✉email: pierre-pol.liebgott@mio.osupytheas.fr

chemolithoautotrophic types of metabolism, using  $H_2$ ,  $H_2S$  or  $CH_4$  as energy sources and oxidized molecules such as oxygen, sulfur compounds, iron oxide or even nitrate as electron acceptors.

However, the discovery of the presence of an abiotic electric current across the conductive pyrite chimney walls<sup>7</sup>, by oxidation of  $H_2S$  inside the chimney and reduction of  $O_2$  outside, prompted the hypothesis of a new type of microorganism called “eletrotrophs”. These microorganisms have the capacity to use electrons from the abiotic electric current as an energy source coupled with carbon fixation from  $CO_2$ . This metabolism was identified a few years ago on a mesophilic chemolithoautotrophic Fe(II)-oxidizing bacterium, *Acidithiobacillus ferrooxidans*<sup>8</sup>. The mechanism of energy uptake from electrodes has been discussed since the discovery of biofilms growing on cathodes, and little is known about this process, unlike that of anodic electron transfer. The two main hypotheses are the use of similar direct electron transfer pathway as on the anode<sup>9</sup>, or the use of free cell-derived enzymes, which can interact with electrode surfaces to catalyze the electron transfers<sup>10</sup>. Recent studies have shown the exoelectrogenic ability of some hyperthermophilic microorganisms isolated from deep-sea hydrothermal vents belonging to *Archaeoglobales* and *Thermococcales*<sup>11–13</sup>, but no studies have been done on environmental samples potentially harboring electro-trophic communities growing naturally with an electric current as their sole energy source.

In this article, we investigate the potential presence of electro-trophic communities in deep-sea hydrothermal vents capable of using electrons directly or indirectly from the abiotic current. To this end, we mimicked the conductive surface of the hydrothermal chimney in a cathodic chamber of Microbial Electrochemical Systems (MESs) with a polarized cathode to enrich the potential electro-trophic communities inhabiting these extreme environments. The polarized cathode served as the sole energy source, while  $CO_2$  bubbling served as sole carbon source. Under these experimental conditions, the distinct effects of the presence of nitrate, oxygen, and sulfate on the community taxonomic composition were investigated.

## Results

**Current consumption from electro-troph enrichment.** Hydrothermal vents chimney samples were inoculated in MESs filled with sterile mineral medium and incubated at 80 °C to enrich electro-trophic communities. The electrode (cathode) and the sparged  $CO_2$  were used as sole energy donor and carbon source, respectively. Nitrate, sulfate and oxygen were separately tested as electron acceptor. The electrode potential has been chosen in order to prevent the abiotic cathodic reduction of the culture medium (Supplementary Fig. S1), thus the electrode was poised at – 590 mV/SHE in the presence of sulfate and nitrate as electron acceptors while this potential was – 300 mV/SHE in the presence of oxygen as electron acceptor. A fourth experiment with sulfate as electron acceptor at – 300 mV/SHE provides information about the effect of the cathode potential on the microbial community. For comparison, microbial growth was also monitored in an inoculated system without any poised electrode during a month in the same incubation conditions. In the latter condition, without an electrode as energy source, no microbial growth occurred, a finding supported by microscope and spectrophotometric observations (data not shown). Moreover, no organic compounds were produced, supported by the HPLC and NMR measurements.

When the electrode was poised, abiotic controls containing no inoculum displayed constant currents of  $\approx 0.016 \text{ A m}^{-2}$  at – 590 mV and  $\approx 0.01 \text{ A m}^{-2}$  at – 300 mV/SHE. In both conditions, no hydrogen production on the cathode via water electrolysis, continuously monitored by  $\mu\text{GC}$ , was detected. The detection threshold of the  $\mu\text{GC}$  ( $>0.001\%$  of total gas) indicated a theoretical production lower than  $34 \mu\text{M day}^{-1}$  (data not shown) as previously reported at 25 °C<sup>14,15</sup>. In comparison, experiments with the chimney sample showed current consumptions increasing shortly after inoculation (Fig. 1). Indeed, when subtracting abiotic current, the current consumptions reached a stabilized maximum of  $0.36 \text{ A m}^{-2}$  on oxygen,  $0.72 \text{ A m}^{-2}$  on nitrate, and up to  $1.83 \text{ A m}^{-2}$  on sulfate at – 590 mV or  $0.76 \text{ A m}^{-2}$  on sulfate at – 300 mV/SHE (data not shown), corresponding to 36, 45, 114 and 76-fold increases compared to abiotic current, respectively. MESs were then autoclaved, displaying decreased currents that were similar to the values of abiotic controls with a stabilized current around  $\approx 0.021 \text{ A m}^{-2}$ , indicating the importance of the living biofilm in the current consumption.

At the end of monitoring of current consumption, CycloVoltamograms (CVs) were performed to study reactions of oxidation and reduction that could occur in MESs (Supplementary Fig. S2A). A first peak of reduction is observed at – 0.295, – 0.293 and – 0.217 V vs SHE in presence of nitrate, sulfate and oxygen as electron acceptor, respectively (Supplementary Fig. S2B). A second peak is observed at – 0.639 and – 0.502 V vs SHE on nitrate and sulfate, respectively. The on-set potential of  $H_2$  evolution was measured in our conditions at – 0.830, – 0.830, – 0.780 and – 0.830 V vs SHE in presence of nitrate, sulfate and oxygen as electron acceptor and in abiotic condition, respectively. No redox peaks were detected in the abiotic controls and freshly inoculated MESs, hence indicating a lack of electron shuttles brought with the inoculum (Supplementary Fig. S2A).

**Organic compounds production in liquid media.** During enrichment of the electro-trophic communities, the production of organic compounds was monitored in the liquid media. Data in presence of Nitrate, Oxygen and Sulfate as electron acceptors at – 300 mV and/or – 590 mV vs SHE are presented in Fig. 1. Glycerol, pyruvate, and acetate were the dominant products released in all experimental runs. Glycerol increased slowly throughout the experiments to reach a maximum of 0.47 mM on sulfate (Day 11, at – 540 mV) or 0.66 mM on sulfate (Day 14, at 300 mV), 1.32 mM on oxygen (Day 12) and 2.32 mM on nitrate (Day 19). Acetate accumulated in the medium to reach 0.33 mM on oxygen (Day 7), 0.75 mM on sulfate (Day 13, at – 590 mV) or 0.34 mM on sulfate (Day 24, at – 300 mV) and 1.40 mM on nitrate (Day 19). Pyruvate was exponentially produced after a few days of culture, reaching a maximum of 1.32, 2.39, and 3.94 mM or 1.79 mM in presence of oxygen (Day 12), nitrate (Day 9), and sulfate (Day 11, at – 590 mV or Day 14, at – 300 mV), respectively. Pyruvate levels varied thereafter, due probably to microbial consumption or thermal degradation. Coulombic efficiency calculated

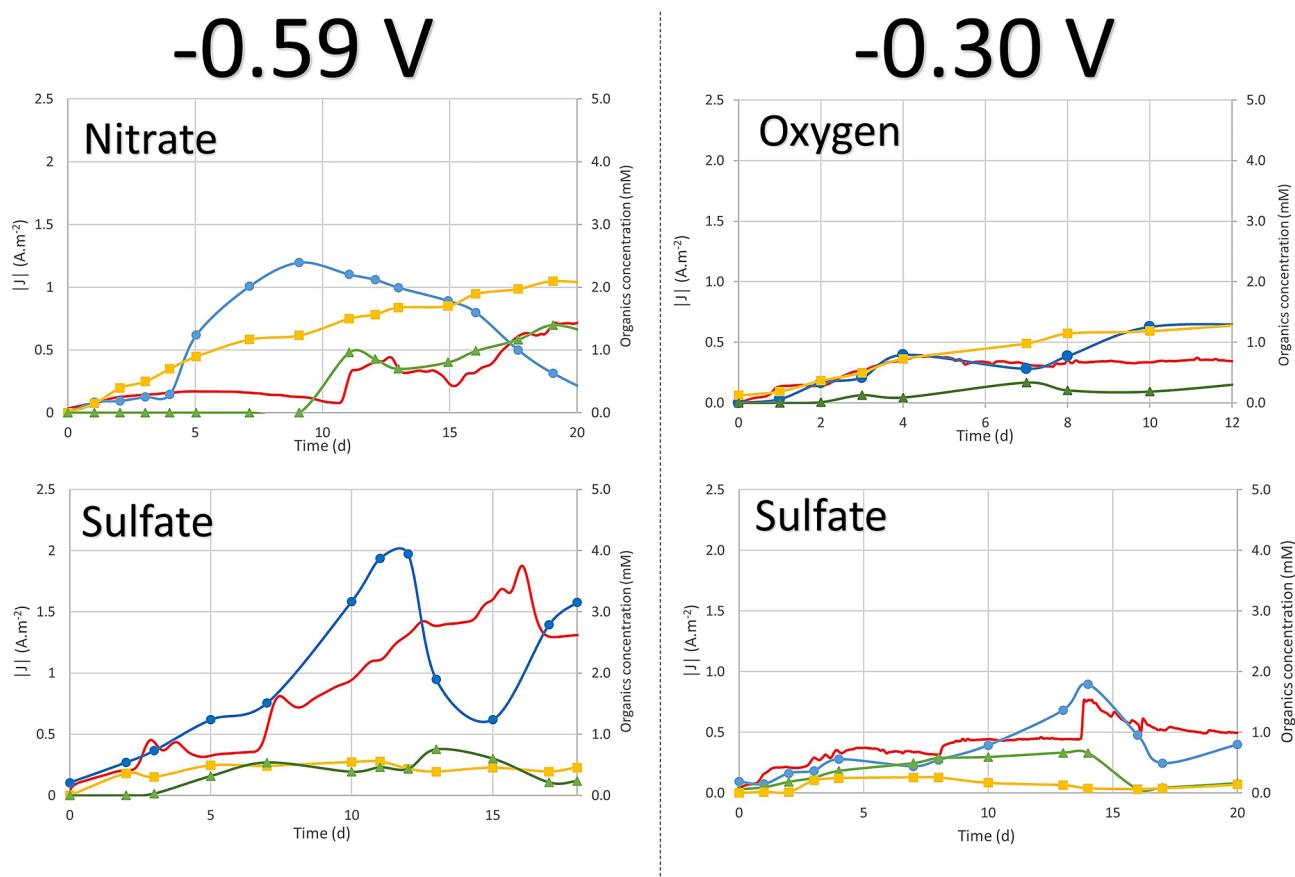


**Figure 1.** Current consumption (red continuous line); pyruvate (blue circle), glycerol (yellow square) and acetate (green triangle) productions over time of culture for each electron-acceptor experiment. The current was obtained from a poised electrode at  $-590$  mV vs SHE for nitrate and sulfate experiments and  $-300$  mV vs SHE for oxygen and sulfate.

on the last day of the experiment (Fig. 2) showed up to 71% (on nitrate), 89% (on oxygen) and 90% (on sulfate, at  $-590$  mV) or 60% (on sulfate, at  $-300$  mV) of electrons consumed were converted to organic compounds and released into the liquid media. The rest represents the share of electrons retained in non-accumulated compounds (Supplementary Table S1) and in the organic matter constituting the cells of the electrothrophic communities (estimated by qPCR to total between  $10^8$  and  $10^{10}$  16S rRNA gene copies per MES Fig. 3).

**Biodiversity of electrothrophic communities on different electron acceptors.** Once current consumption reached a stabilized maximum, gDNAs from the biofilm (found on the cathode) and from planktonic cells (found in liquid media) were extracted and sequenced on the V4 region of the 16S rRNA to study relative biodiversity. Figure 3 reports the taxonomic affiliation of the OTUs obtained with nitrate, sulfate or oxygen as electron acceptors.

The chimney fragment inoculum showed a rich biodiversity (Shannon index at 5.29 and Pielou's index at 0.69), with 208 OTUs mainly affiliated to *Bacteria* (99.49% vs 0.51% of *Archaea*) and more particularly to *Proteobacteria* from *Vibrionales* (34.8%), miscellaneous rare *Proteobacteria* (> 33%), *Campylobacteriales* (8.3%), *Thermales* (7.1%), *Aquificales* (5.62%), and *Rhodobacteriales* (5.1%).

Enrichments in MES showed less biodiversity in biofilms and in liquid media (planktonic cells), suggesting the selective development of functional communities. The Shannon index values in biofilms and liquid media respectively, were 3.1 and 1.9 on nitrate, 1.7 and 1.9 on sulfate (2.3 and 2.2 on sulfate at  $-300$  mV), and 4.1 and 4.2 on oxygen, with fewer OTUs associated to 72 and 68 OTUs on nitrate, 39 and 53 on sulfate (62 and 57 on sulfate, at  $-300$  mV), and 94 and 102 on oxygen. The taxonomic composition of these communities showed a larger proportion of *Archaea*, with 51% and 41.6% on nitrate, 96.7% and 97.4% on sulfate (90.3% and 90.9%, at  $-300$  mV), and 7.5% and 3.3% on oxygen, in biofilms and in liquid media, respectively. Whatever the electron acceptor used, the archaeal population in biofilms, was mainly composed of *Archaeoglobales* and *Thermococcales* at different relative abundances. These were present at proportions ranging from 6.6% and 28.2% on nitrate to 65.2% and 28.8% on sulfate (54.9% and 30.2% at  $-300$  mV) and 3.7% and 3.1% on oxygen, for *Archaeoglobales* and *Thermococcales* respectively. Equivalent proportions of *Archaeoglobales* and *Thermococcales* were retrieved in liquid media, at 1.0% and 2.5% on nitrate as electron acceptor, 64.8% and 30.7% on sulfate as electron acceptor (58.9% and 30.9%, at  $-300$  mV) and 0.2% and 3.1% on oxygen as electron acceptor, respectively (see Fig. 3). The

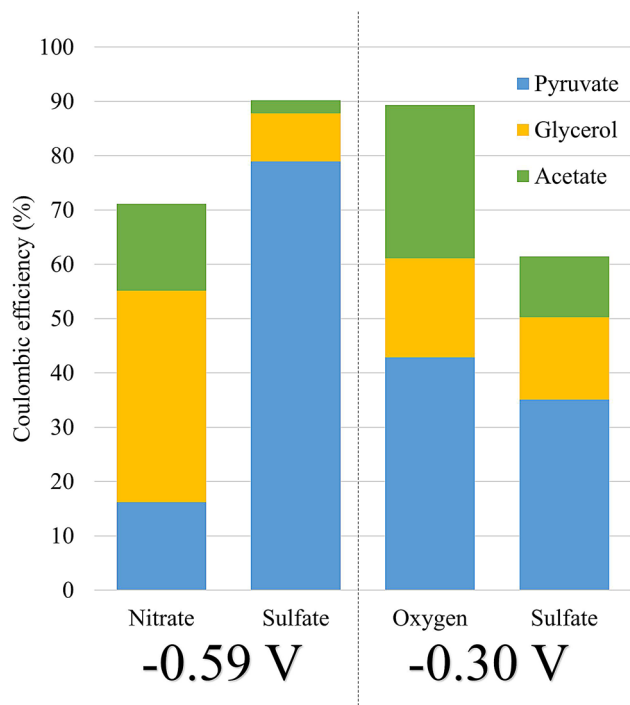


**Figure 2.** Coulombic efficiency for organic products in presence of the different electron acceptors.

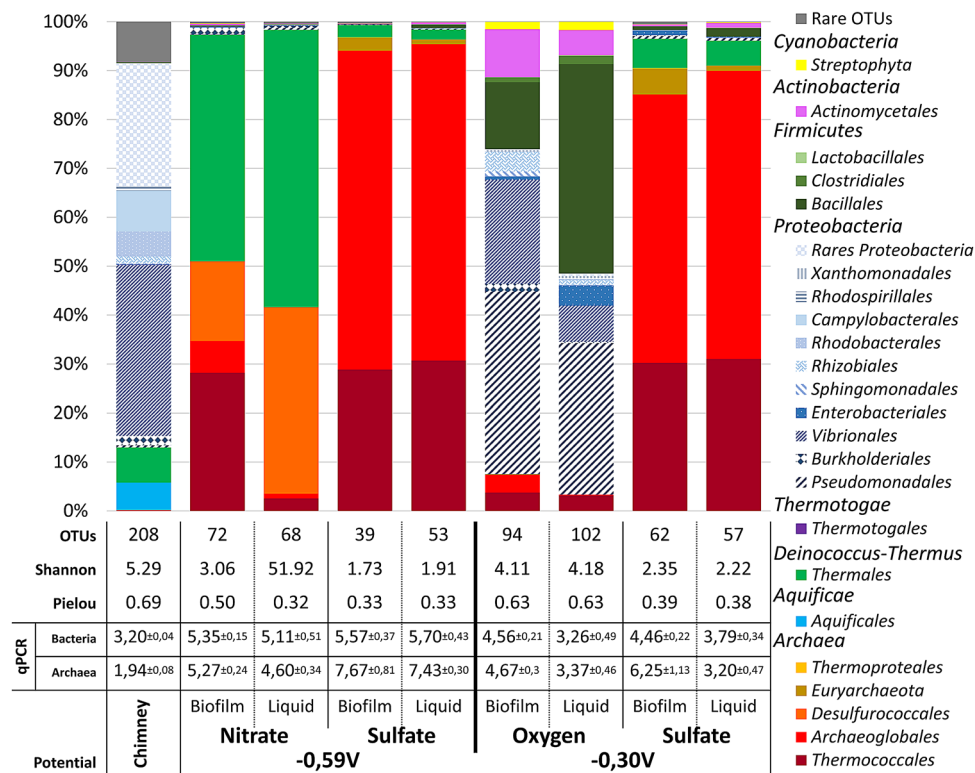


**Figure 3.** Dominant taxonomic affiliation at order level, biodiversity indices and qPCR of microbial communities from a crushed chimney sample from Capelinhos vent site (Lucky Strike hydrothermal vent field), as plotted on the cathode and liquid media after the weeks of culture. OTUs representing less than 1% of total sequences of the samples are pooled as ‘Rare OTUs’. qPCR expressed in Log<sub>10</sub> Cells per gram of crushed chimney (Chimney), per milliliter of liquid (Liquid: planktonic cells) or per cm<sup>2</sup> of electrode/cathode (Biofilm). Standard deviation obtained on analytical triplicates.



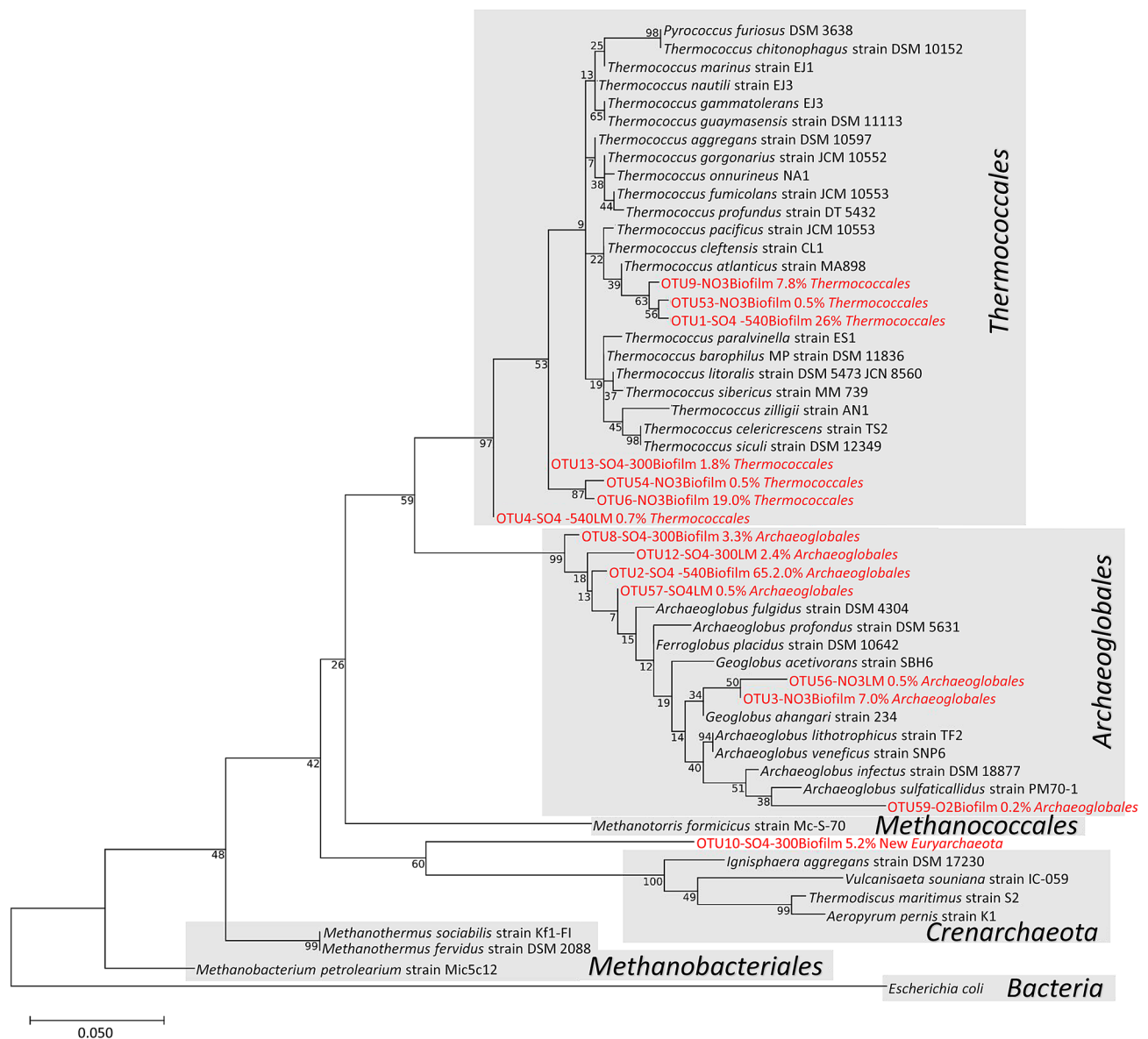


**Figure 4.** Maximum Likelihood phylogenetic tree of archaeal OTUs retrieved on various enrichments on the 293bp 16S fragment obtained in the barcoding 16S method (LM: Liquid Media/planktonic cells). Numbers at nodes represent bootstrap values inferred by MEGAX. Scale bars represent the average number of substitutions per site. This phylogenetic tree was obtained with MEGAX<sup>52</sup> software v10.0.5 (<https://www.megasoftware.net/>) with the MUSCLE alignment algorithm and Inferring of the Maximum Likelihood Tree with a Bootstrap test (2500 replications).

MiSeq Illumina results served to study only 290 bp of 16S rRNA and thus to affiliate microorganisms confirmed at the family level, but they can also provide some information on the enriched genera.

To obtain more information on the probable *Archaeoglobales* and *Thermococcales* genus, we attempted a species-level identification through phylogenetic analysis. The results are presented in Fig. 4 as a Maximum likelihood phylogenetic tree.

The dominant OTUs on sulfate and oxygen as electron acceptors, were closest to *Ferroglobus placidus* and *Archeoglobus fulgidus* (97.6% of identity), whereas the dominant OTU on nitrate was affiliated to *Geoglobus ahangari* with an identity of 98.63%. The remaining part of the biodiversity was specific to each electron acceptor used. Enrichment on nitrate showed 16.2% and 38.1% of *Desulfurococcales* and 46.4% and 56.7% of *Thermococcales* in the biofilm and in the liquid medium, respectively. Among *Thermococcales* that developed on the electrode with nitrate as electron acceptor, 30% were represented by a new taxon (OTU 15 in Supplementary Fig. S3) whose closest cultured species was *Vulcanithermus mediatlanticus* (90% of identity). On sulfate, the remaining biodiversity represented less than 4% (at – 590 mV) and 10% (at – 300 mV) of the population but was mainly represented by two particular OTUs. The first OTU was affiliated to a new *Euryarchaeota* and accounted for up to 2.6% and 0.9% of the total population in the biofilm and in the liquid medium (5.2% and 1.0% at – 300 mV), respectively

(OTU 10 in Fig. 4 and Supplementary Fig. S3). The closest cultured match (86% of identity) was *Methanothermus fervidus* strain DSM 2088. The second OTU was affiliated to the new *Thermales* species found in the nitrate condition and accounted in sulfate enrichment for 2.5% and 2.0% of the biodiversity (6.0% and 5.1%, at  $-300$  mV) on the electrode and in liquid media, respectively (OTU 15 in Supplementary Fig. S3). In the enrichment on oxygen, the communities were dominated by 37.2% and 30.9% of *Pseudomonadales* (*Pseudomonas* sp.), 13.7% and 42.8% of *Bacillales* (*Bacillus* and *Geobacillus* sp.), 21.3% and 7.4% of *Vibrionales* (*Photobacterium* sp.), and 9.8% and 5.1% of *Actinomycetales* (spread across 9 species) in the biofilm and in the liquid medium, respectively. The remaining biodiversity was spread across *Proteobacteria* orders.

The clustering of the dominant OTUs (at a threshold of 0.5% of total sequences) obtained previously on the chimney sample and enrichments in MES showed a clear differentiation of communities retrieved in each sample (Supplementary Fig. S3). The Pearson method used on OTU distribution produced four clusters, one corresponding to the inoculum and the three others to each electron acceptor regardless of used potentials during  $\text{SO}_4$  condition. Indeed, only two OTUs (OTU4 and 51) were clearly shared between two different communities, affiliated to *Thermococcus* spp. on nitrate and sulfate and to *Bacillus* sp. on oxygen and on sulfate. The other 49 dominant OTUs were specific to one community, with 21 OTUs on oxygen, 6 on sulfate, 8 on nitrate, and 14 on the chimney sample. The same OTUs were retrieved in the two individual Sulfate enrichments, suggesting specificity of these OTUs to the electron acceptor rather than random expansion of OTUs from the inoculum. The electro-trophic communities colonizing the cathode were therefore different depending on electron acceptor used and their concentration was too low to be detected in the chimney sample.

## Discussion

**Archaeoglobales as systematic (electro)lithoautotrophs of the community.** We have evidenced the development of microbial electro-trophic communities and metabolic activity supported by current consumption (Fig. 1), product production (Fig. 2), and qPCRs (Fig. 3). These data suggest that growth did occur from energy supplied by the cathode. Our study is the first to show the possibility of growth of biofilm from environments harboring natural electric current in the total absence of soluble electron donors. To further discuss the putative mechanism, it is necessary to have a look at our conditions unfavorable for water electrolysis (see Supplementary Fig. S2). The equilibrium potential for water reduction into hydrogen at  $80^\circ\text{C}$ , pH 7, and 1 atm was calculated at  $-0.490$  V vs SHE in pure water. The operational reduction potential is expected to be lower than the theoretical value due to internal resistances (from electrical connections, electrolytes, ionic membranes, etc.)<sup>16</sup> and overpotentials (electrode material). This was confirmed with the on-set potential of  $\text{H}_2$  evolution measured at  $-0.830$  mV vs SHE in both experimental condition and abiotic control, indicating the absence of catalytic effect of putative hydrogenases secreted by the biofilm or metals from inoculum. Also, during preliminary potentials screening, the increase in current consumption and  $\text{H}_2$  production was observed only below  $-0.7$  V vs SHE (Supplementary Figs. S1 and S2). In addition, the presence of catalytic waves observed by CV with midpoint potentials between  $-0.217$  V to  $-0.639$  V indicate the implication of enzymes directly connected to the surface of the electrode (see Supplementary Fig. S2). Finally, the fixation of 267–1596 Coulombs  $\text{day}^{-1}$  into organics (Fig. 1) exceeds the maximum theoretical abiotic generation of hydrogen from abiotic current ( $\sim 3$  C  $\text{day}^{-1}$ ) 90- to 530-fold<sup>17</sup>.

Therefore, under our experimental conditions, the biofilm growth should be largely ensured by a significant part of a direct transfer of electrons from the cathode, thereby demonstrating the presence of electro-lithoautotroph microorganisms. This is supported by obtaining a similar biodiversity on sulfate with the cathode poised at  $-300$  mV [compared to  $-590$  mV vs SHE (Fig. 3)], whose potential is 190 mV more positive than the Equilibrium potential of  $\text{H}_2$  evolution ( $-490$  mV vs SHE), with then no electrochemical possibility of  $\text{H}_2$  production, even at molecular level.

Taxonomic analysis of the enriched microbial communities at the end of the experiments showed the systematic presence of *Archaeoglobales* on cathodes. Moreover, the qPCR and MiSeq data (Fig. 3) highlighted a strong correlation between current consumption and density of *Archaeoglobales* in the biofilm (Supplementary Fig. S4,  $R^2=0.945$ ).

The OTUs were related to some *Archaeoglobales* strains with 95–98% identities. Thus, we assume that under our experimental conditions new specific electro-trophic metabolisms or new electro-lithoautotrophic *Archaeoglobaceae* species were enriched on the cathode. They were retrieved in all conditions and belonged to the only order in our communities exhibiting autotrophic metabolism. Autotrophic growth in the *Archaeoglobales* order is ensured mainly through using  $\text{H}_2$  as energy source and requires both branches of the reductive acetyl-CoA/Wood-Ljungdahl pathway for  $\text{CO}_2$  fixation<sup>18</sup>. Terminal electron acceptors used by this order include sulfate, nitrate, poorly crystalline Fe (III) oxide, and sulfur oxyanions<sup>19</sup>. Moreover, *Archaeoglobus fulgidus* has been recently shown to grow on iron by directly snatching electrons under carbon starvation during the corrosion process<sup>20</sup>. Furthermore, *Ferroglobus* and *Geoglobus* species were shown to be exoelectrogens in pure culture in a microbial electrosynthesis cell<sup>12</sup> and have been enriched within a microbial electrolysis cell<sup>11,13</sup>. Given these elements, the identified *Archaeoglobales* species could be, under our electro-lithoautotrophic conditions, the first colonizers of the electrode during the first days of growth. This hypothesis was confirmed into a more detailed study focusing on the enrichment on nitrate<sup>21</sup>.

The growth of *Archaeoglobales* species in presence of oxygen is a surprising finding. *Archaeoglobales* have a strictly anaerobic metabolism, and the reductive acetyl-CoA pathway is very sensitive to the presence of oxygen<sup>22</sup>. This can be firstly explained by the low solubility of oxygen at  $80^\circ\text{C}$ . Secondly, carbon cloth mesh reduces oxygen in the environment, allowing for anaerobic development of microorganisms into a protective biofilm<sup>23</sup>. This observation was supported by the near absence of *Archaeoglobales* in the liquid medium (Fig. 3). One of the hypotheses concerns direct interspecies electron transfer (DIET)<sup>24,25</sup>, with *Archaeoglobales* transferring

electrons to another microorganism as an electron acceptor. Research into DIET is in its early stages, and further investigations are required to better understand the diversity of microorganisms and the mechanism of carbon and electron flows in anaerobic environments<sup>25</sup> such as hydrothermal ecosystems.

**Electrosynthesis of organic compounds.** Accumulation of pyruvate, glycerol and acetate was measured, while another set of compounds that appeared transiently were essentially detectable in the first few days of biofilm growth (Supplementary Table S1). They included amino acids (threonine, alanine) and volatile fatty acids (formate, succinate, lactate, acetoacetate, 3-hydroxyisovalerate) whose concentrations did not exceed 0.1 mM. Despite their thermostability, this transient production suggests they were used by microbial communities developing on the electrode in interaction with the primary producers during enrichment.

On the other hand, in presence of nitrate, sulfate and oxygen as electron acceptors, the liquid media accumulated mainly acetate, glycerol, and pyruvate (Fig. 1). Coulombic efficiency calculations (Fig. 2) showed that electron content of the carbon products represented 60–90% of electrons consumed, the rest being potentially used directly for biomass or transferred to an electron acceptor. This concurs with the energy yield from the Wood-Ljungdahl pathway of *Archaeoglobales*, with only 5% of carbon flux directed to the production of biomass and the other 95% diverted to the production of small organic end-products excreted from the cell<sup>26</sup>.

Pyruvate is a central intermediate of CO<sub>2</sub> uptake by the reducing pathway of the acetyl-CoA/WL pathway<sup>27</sup>. It can be used to drive the anabolic reactions needed for biosynthesis of cellular constituents. Theoretically, the only explanation for improved production and accumulation of pyruvate (up to 5 mM in the liquid media of sulfate experiment) would be that pyruvate-consuming enzymes were inhibited or that pyruvate influx exceeded its conversion rate. Here we could suggest that in-cell electron over-feeding at the cathode leads to significant production of pyruvate when the electron acceptor runs out.

In an ecophysiological context, similar pyruvate and glycerol production could occur on hydrothermal chimney walls into which electric current propagates<sup>28</sup>. The electrotoph biofilms would continually receive electrons, leading to an excess of intracellular reducing power which would be counterbalanced by overproduction of glycerol and pyruvate<sup>29,30</sup>. Furthermore, these products can serve as carbon and energy sources for heterotrophic microorganisms or for fermentation. In our experiments, pyruvate and glycerol concentrations varied over time, suggesting they were being consumed by heterotrophic microorganisms. Acetate production would thus result from the fermentation of pyruvate or other compounds produced by electrotoph *Archaeoglobales*.

*Enrichment of rich heterotrophic biodiversity from electrotoph *Archaeoglobales* community.* During our enrichment experiments, the development of effective and specific biodiversity was dependent on the electron acceptors used (Fig. 3). Heatmap analyses (Supplementary Fig. S3) showed four distinct communities for the three electron acceptors and the initial inoculum. Thus, at the lower taxonomic level of the biodiversity analysis, most OTUs are not common to multiple enrichments, except for one OTU of *Thermococcales* that was found in both the nitrate and sulfate experiments. This suggests a real specificity of the communities and a specific evolution or adaptation of the members of the shared phyla to the different electron acceptors available in the environment. However, the various enrichments also showed the presence of *Thermococcales* regardless of the electron acceptors used, thus demonstrating a strong interaction between *Thermococcales*, assumed to be heterotrophs, and *Archaeoglobales*, the only demonstrated autotrophs. Moreover, members of these two groups have frequently been found together in various hydrothermal sites<sup>4,5,31,32</sup>, where they are considered potential primary colonizers<sup>33–37</sup>. After *Thermococcales*, the rest of the heterotrophic biodiversity was specific to each electron acceptor.

On nitrate, two additional phylogenetic groups were retrieved: *Desulfurococcales* and *Thermales*. OTUs of *Desulfurococcales* are mainly affiliated to *Thermodiscus* or *Aeropyrum* species, which are hyperthermophilic and heterotrophic *Crenarchaeota* growing by fermentation of complex organic compounds or sulfur/oxygen reduction (Huber and Stetter, 2015). Concerning *Thermales*, a new taxon was enriched on cathode and only affiliated to *Vulcanithermus mediatlanticus* with similarity of 90%. This new taxon of *Thermales* (OTU 15, Supplementary Fig. S3) was also enriched up to 2% on the cathode of sulfate enrichment. *Thermales* are thermophilic (30–80 °C) and heterotrophic bacteria whose only four genera (*Marinithermus*, *Oceanithermus*, *Rhabdothermus*, and *Vulcanithermus*) are all retrieved in marine hydrothermal systems. They can grow under aerobic, microaerophilic and some anaerobic conditions with several inorganic electron acceptors such as nitrate, nitrite, Fe (III) and elemental sulfur<sup>38</sup>. All of the *Thermales* species can utilize the pyruvate as carbon and energy source with the sulfate or nitrate as electron acceptors.

*Pseudomonadales* and *Bacillales* were found in the oxygen experiment. Most *Pseudomonas* are known to be aerobic and mesophilic bacteria, with a few thermophilic species (up to 65 °C)<sup>39,40</sup>. There have already been some reports of mesophilic *Pseudomonas* species growing in thermophilic conditions in composting environments<sup>41</sup>. Moreover, some *Pseudomonas* sp. are known to be electroactive in microbial fuel cells through long-distance extracellular electron transport<sup>42–44</sup>, and were dominant on the cathodes of a benthic microbial fuel cell on a deep-ocean cold seep<sup>45</sup>. In *Bacillales*, the *Geobacillus* spp. and some *Bacillus* sp. are known to be mainly (hyper) thermophilic aerobic and heterotrophic *Firmicutes*<sup>46</sup>.

*Hydrothermal electric current: a new energy source for the development of primary producers.* The presence of so many heterotrophs in an initially autotrophic condition points to the hypothesis of a trophic relationship inside the electrotoph community (Fig. 5). This suggests that the only autotrophs retrieved in all communities, the *Archaeoglobales*, might be the first colonizer of the electrode, using CO<sub>2</sub> as carbon source and the cathode as energy source. Models using the REACT module of the Geochemist's Workbench (GWB) and based on electron donor acceptor availability predicted low abundances of *Archaeoglobales* (<0.04%) due to low concentration of



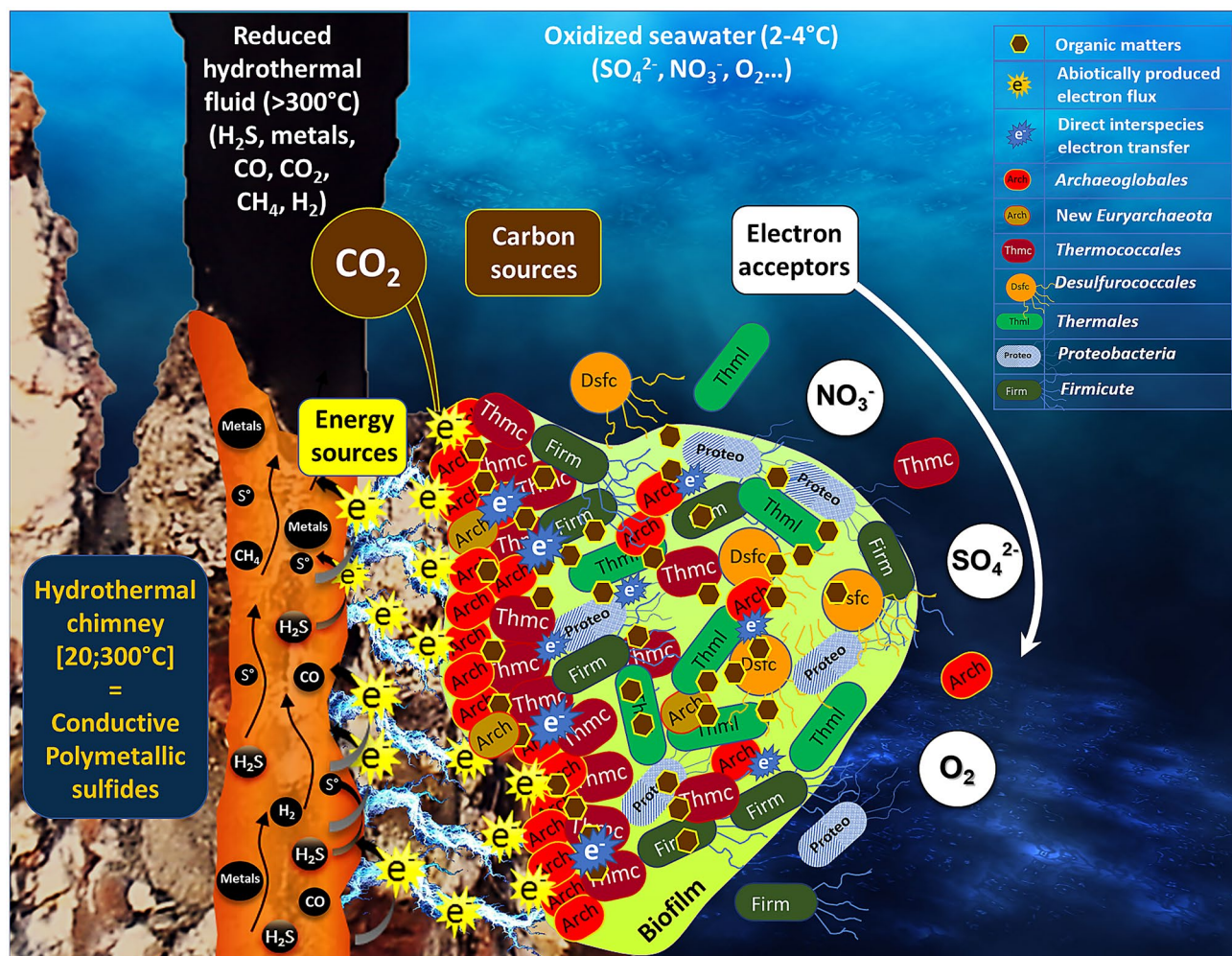


**Figure 5.** Schematic representation of microbial colonization of iron-rich hydrothermal chimney (Capelinhos site on the Lucky Strike hydrothermal field) by electrolithoautotrophic microorganisms. The production of an abiotic electrical current by potential differences between the reduced hydrothermal fluid ( $\text{H}_2\text{S}$ , metals,  $\text{CO}$ ,  $\text{CH}_4$ ,  $\text{H}_2$ ...) and oxidized seawater ( $\text{O}_2$ ,  $\text{SO}_4^{2-}$ ,  $\text{NO}_3^-$ ) (Yamamoto et al.<sup>28</sup>) leads to the formation of electron flux moving towards the chimney surface. This electrons flux can serve directly as an energy source to enable the growth of electrolithoautotrophic and hyperthermophilic Archaeoglobales using the  $\text{CO}_2$  as carbon source and nitrate and/or sulfate as electron acceptors. In the absence of a usable electron acceptor, Archaeoglobales would be likely to perform direct interspecies electron transfer to ensure their growth. The electron acceptor fluctuations, correlated to the continual influx of electric current would favor the production of organic matters (amino acid, formate, pyruvate, glycerol...) by the Archaeoglobales. This organic matter is then used by heterotrophic microorganisms by fermentation or respiration (anaerobic or aerobic) thus providing the primal food web initially present into the hydrothermal ecosystems. The electrical current also could favor the electrolysis water leading to the abiotic  $\text{H}_2$  production (not measurable in our abiotic conditions), which would serve as chemical energy source. *Arch* Archaeoglobales, *Thmc* Thermococcales, *Dsfc* Desulfurococcales, *Thml* Thermales, *Prot* Proteobacteria, *Firm* Firmicute,  $\text{NO}_3^-$  nitrate,  $\text{SO}_4^{2-}$  sulfate,  $\text{O}_2$  dioxygen,  $\text{CH}_4$  Methane,  $\text{CO}_2$  Carbon Dioxide,  $\text{CO}$  Carbon monoxide,  $\text{H}_2\text{S}$  Hydrogen sulfide,  $\text{S}^0$  sulfur; Metals: Fe, Mn, Cu, Zn.

$\text{H}_2$ <sup>36</sup> whereas in-situ detection found abundances of more than 40% in the inner section of the studied hydrothermal chimney<sup>47</sup>. Dahle et al. concluded on a probable  $\text{H}_2$  syntrophy, with hydrogen being produced by heterotrophic microorganisms such as fermentative *Thermococcales* species. Our study showed that Archaeoglobales can also grow electrolithoautotrophically, feeding on the natural electric current through the chimney walls. This new energy source, which is not considered in the models, would gap this model/observation difference and raises the question of the importance of this metabolism in the primary colonization of hydrothermal vents. It would allow a long-range transfer between the electron donor ( $\text{H}_2\text{S}$  oxidized on the inner surface of the chimney wall) and the electron acceptors ( $\text{O}_2$ , sulfur compounds, nitrate, metals) covering the external surface of the chimney. This electrical current would thus allow primary colonizers to grow, releasing organic compounds which are then used by the heterotrophic community, as observed in our experiments. Moreover, this would provide a constant source of electron donor to all over the surface of the chimney, allowing to meet a wider range of physiological conditions through pH, temperature, and oxidoreduction gradients. This allows a wider diversity

of growth patterns than through chemolithoautotrophy, which is restricted to unstable and limited contact zones between reduced compounds ( $H_2$ ,  $H_2S$ ) in the hydrothermal fluid and electron acceptors around the hydrothermal chimneys ( $O_2$ ,  $SO_4$ ,  $NO_3$ ), which often precipitate together.

## Conclusion

Taken together, the results found in this study converge into evidence of the ability of indigenous microorganisms from deep hydrothermal vents to grow autotrophically ( $CO_2$  used as only carbon source) using electric current as energy source. This ability seems to be spread across diverse phylogenetic groups and to be coupled with diverse electron acceptors. Through their electro-litho-auto-trophic metabolism, *Archaeoglobaceae* strains could produce and release organic compounds into their close environment, allowing the growth of heterotrophic microorganisms and ultimately enabling more and more diversity to develop over time (Fig. 5). This metabolism could be one of the primary energies for the colonization of deep-sea hydrothermal chimneys and the development of a complex trophic network driving sustainable biodiversity. A similar direct electron-uptake mechanism could have occurred in the hydrothermal vents of the Hadean, allowing the emergence of life in hydrothermal environments through constant electron influx to the first proto-cells.

## Methods

**Sample collection and preparation.** A hydrothermal chimney sample was collected on the acidic and iron-rich Capelinhos site on the Lucky Strike hydrothermal field ( $37^\circ 17.0' N$ , MAR) during the MoMARsat cruise in 2014 (<http://dx.doi.org/10.17600/14000300>) led by IFREMER (France) onboard R/V *Pourquoi Pas?*<sup>48</sup>. The sample (PL583-8) was collected by breaking off a piece of a high-temperature active black smoker using the submersible's robotic arm and bringing it back to the surface in a decontaminated insulated box (<http://video.ifremer.fr/video?id=9415>). Onboard, chimney fragments were anaerobically crushed in an anaerobic chamber in an  $H_2:N_2$  (2.5:97.5) atmosphere (La Calhene, France), placed in flasks under anaerobic conditions (anoxic seawater at pH 7 with  $0.5 \text{ mg L}^{-1}$  of  $Na_2S$  and  $N_2:H_2:CO_2$  (90:5:5) gas atmosphere), and stored at  $4^\circ C$ .

Prior to our experiments, pieces of the hydrothermal chimney were removed from the sulfidic seawater flask, crushed with a sterile mortar and pestle in an anaerobic chamber (Coy Laboratories, Grass Lake, MI), and distributed into anaerobic tubes for use in the various experiments.

**Electrotrophic enrichment on nitrate, sulfate, and oxygen.** MESs, composed of 2 H-cell chambers of 2 L each separated with a anionic membrane (AMI, Membrane International) of 10 cm of diameter, as previously described<sup>13</sup>. The chambers were filled with 1.5 L of an amended sterile mineral medium<sup>13</sup> without yeast extract and set at  $80^\circ C$  and pH 6.0 through on-platform monitoring. The electrode (cathode), composed of  $20 \text{ cm}^2$  of carbon cloth, was poised at the lowest potential before initiation of abiotic current consumption (Supplementary Fig. S4) using SP-240 potentiostats and EC-Lab software (BioLogic, France). Potentials were considered for pH 6.0 and  $80^\circ C$  vs SHE. A potential of  $-590 \text{ mV}$  vs SHE was used in the nitrate and sulfate experiments and  $-300 \text{ mV}$  vs SHE in the oxygen experiment. A similar experiment at  $-300 \text{ mV}$  vs SHE has been initiated in presence of sulfate (Fig. 3) to confirm the growth of electrolithoautotroph communities at lower potential, avoiding potential  $H_2$  production. The electrode poised as cathode served as the sole electron donor for electrotroph growth. For nitrate and sulfate experiments, the MES was supplemented with 4 mM of sodium nitrate or 10 mM of sodium sulfate, respectively. The cathodic chambers were sparged with  $N_2:CO_2$  (90:10, 100 mL/min) and equipped with a condenser to avoid evaporation. For the oxygen experiment, the MES was sparged with  $N_2:CO_2:O_2$  (80:10:10, 100 mL/min) with initially 10% oxygen as electron acceptor. All experiments were inoculated with 8 g of the crushed chimney [ $\sim 0.5\%$  (w/v)]. Current consumption was monitored via the chronoamperometry method. An abiotic control without inoculation showed no increase of current consumption during the same experiment period. At the end of the experiment, half of the electrode and some liquid media were collected for analysis. The rest was autoclaved and the current consumption was monitored again after sterilization for few days. CycloVoltammograms (scan rate:  $20 \text{ mV/s}$ ) were analyzed using QSoas software (version 2.1). Coulombic efficiencies were calculated using the following equation:

$$CE(\%) = \frac{F \cdot n_e \cdot \Delta[P] \cdot V_{\text{catholyte}}}{\int_{t_0}^t I(t) \cdot dt} \cdot 100.$$

$I(t)$  is the current consumed between  $t_0$  and  $t$  (A),  $F$  is the Faraday constant,  $n_e$  is the number of moles of electrons presents per mole of product (mol),  $\Delta[P]$  is the variation of the concentration of organic product between  $t_0$  and  $t$  (mol/L),  $V_{\text{catholyte}}$  is the volume of catholyte (L).

**Identification and quantification of organic compound production.** To identify and quantify the production of organic compounds from the biofilm, samples of liquid media were collected at the beginning and at the end of the experiment and analyzed by  $^1H$  NMR spectroscopy. For this, 400  $\mu L$  of each culture medium were added to 200  $\mu L$  of PBS solution prepared in  $D_2O$  ( $NaCl$ , 140 mM;  $KCl$ , 2.7 mM;  $KH_2PO_4$ , 1.5 mM;  $Na_2HPO_4$ , 8.1 mM; pH 7.4) supplemented with 0.5 mmol/L of trimethylsilylpropionic acid-*d4* (TSP) as NMR reference. All the 1D  $^1H$  NMR experiments were carried out at 300 K on a Bruker Avance spectrometer (Bruker, BioSpin Corporation, France) operating at 600 MHz for the  $^1H$  frequency and equipped with a 5-mm BBFO probe.

Spectra were recorded using the 1D nuclear Overhauser effect spectroscopy pulse sequence (Trd- $90^\circ$ - $T_1$ - $90^\circ$ -tm- $90^\circ$ -Taq) with a relaxation delay (Trd) of 12.5 s, a mixing time (tm) of 100 ms, and a  $T_1$  of 4  $\mu s$ . The sequence enables optimal suppression of the water signal that dominates the spectrum. We collected 128 free induction

decays (FID) of 65,536 datapoints using a spectral width of 12 kHz and an acquisition time of 2.72 s. For all spectra, FIDs were multiplied by an exponential weighting function corresponding to a line broadening of 0.3 Hz and zero-filled before Fourier transformation. NMR spectra were manually phased using Topspin 3.5 software (Bruker Biospin Corporation, France) and automatically baseline-corrected and referenced to the TSP signal ( $\delta = -0.015$  ppm) using Chenomx NMR suite v7.5 software (Chenomx Inc., Canada). A 0.3 Hz line-broadening apodization was applied prior to spectral analysis, and  $^1\text{H}$ - $^1\text{H}$  TOCSY (Bax and Davis, 1985) and  $^1\text{H}$ - $^{13}\text{C}$  HSQC<sup>49</sup> experiments were recorded on selected samples to identify the detected metabolites. Quantification of identified metabolites was done using Chenomx NMR suite v7.5 software (Chenomx Inc., Canada) using the TSP signal as the internal standard.

**Biodiversity analysis.** Taxonomic affiliation was carried out according to Ref.<sup>50</sup>. DNA was extracted from 1 g of the crushed chimney and, at the end of each culture period, from scrapings of half of the WE and from centrifuged pellets of 50 mL of spent media. The DNA extraction was carried out using the MoBio PowerSoil DNA isolation kit (Carlsbad, CA). The V4 region of the 16S rRNA gene was amplified using the universal primers 515F (5'-GTG CCA GCM GCC GCG GTA A-3') and 806R (5'-GGA CTA CNN GGG TAT CTA AT-3')<sup>51</sup> with Taq&Load MasterMix (Promega) in triplicates and pooled together. PCR reactions, qPCR, amplicon sequencing and taxonomic affiliation were carried out as previously described<sup>11</sup>. The qPCR results were expressed in number of copies of 16 s rRNA gene per gram of crushed chimney, per milliliter of liquid media or per cm<sup>2</sup> of surface of the electrode. To analyze alpha diversity, the OTU tables were rarefied to a sampling depth of 9410 sequences per library, and three metrics were calculated: the richness component, represented by number of OTUs observed, the Shannon index, representing total biodiversity, and the evenness index (Pielou's index), which measures distribution of individuals within species independently of species richness. Rarefaction curves (Supplementary Fig. S5) for each enrichment approached an asymptote, suggesting that the sequencing depths were sufficient to capture overall microbial diversity in the studied samples. The phylogenetic tree was obtained with MEGAX<sup>52</sup> software v10.0.5 (<https://www.megasoftware.net/>) with the MUSCLE alignment algorithm and inferring of the Maximum Likelihood Tree with a Bootstrap test (2500 replications). The heatmap was obtained using RStudio software v3. The raw sequences for all samples can be found in the Sequence Read Archive (accession number: PRJNA734279).

Received: 23 April 2021; Accepted: 28 June 2021

Published online: 20 July 2021

## References

1. Corliss, J. B. & Ballard, R. D. Oasis of life in the cold abyss. *Nat. Geogr. Mag.* **152**, 440–453 (1977).
2. Alain, K. *et al.* Early steps in microbial colonization processes at deep-sea hydrothermal vents. *Environ. Microbiol.* **6**, 227–241 (2004).
3. Huber, J. A., Butterfield, D. A. & Baross, J. A. Temporal changes in archaeal diversity and chemistry in a mid-ocean ridge subsurface habitat. *Appl. Environ. Microbiol.* **68**, 1585–1594 (2002).
4. Nercessian, O., Reysenbach, A.-L., Prieur, D. & Jeanthon, C. Archaeal diversity associated with in situ samplers deployed on hydrothermal vents on the East Pacific Rise (13°N). *Environ. Microbiol.* **5**, 492–502 (2003).
5. Takai, K. *et al.* Spatial distribution of marine *Crenarchaeota* Group I in the vicinity of deep-sea hydrothermal systems. *Appl. Environ. Microbiol.* **70**, 2404–2413 (2004).
6. Wirth, R., Luckner, M. & Wanner, G. Validation of a hypothesis: Colonization of black smokers by hyperthermophilic microorganisms. *Front. Microbiol.* **9**, 524 (2018).
7. Yamamoto, M., Nakamura, R. & Takai, K. Deep-sea hydrothermal fields as natural power plants. *ChemElectroChem* **5**, 2162 (2018).
8. Ishii, T., Kawauchi, S., Nakagawa, H., Hashimoto, K. & Nakamura, R. From chemolithoautotrophs to electrolithoautotrophs: CO<sub>2</sub> fixation by Fe(II)-oxidizing bacteria coupled with direct uptake of electrons from solid electron sources. *Front. Microbiol.* **6**, 994 (2015).
9. Pous, N. *et al.* Bidirectional microbial electron transfer: Switching an acetate oxidizing biofilm to nitrate reducing conditions. *Biosens. Bioelectron.* **75**, 352–358 (2016).
10. Deutzmann, J. S., Sahin, M. & Spormann, A. M. Extracellular enzymes facilitate electron uptake in biocorrosion and bioelectrosynthesis. *MBio* **6**, e00496-15 (2015).
11. Pillot, G. *et al.* Specific enrichment of hyperthermophilic electroactive *Archaea* from deep-sea hydrothermal vent on electrically conductive support. *Bioresour. Technol.* **259**, 304–311 (2018).
12. Yilmazel, Y. D., Zhu, X., Kim, K.-Y., Holmes, D. E. & Logan, B. E. Electrical current generation in microbial electrolysis cells by hyperthermophilic archaea *Ferroglobus placidus* and *Geoglobus ahangari*. *Bioelectrochemistry* **119**, 142–149 (2018).
13. Pillot, G. *et al.* Production of current by syntrophy between exoelectrogenic and fermentative hyperthermophilic microorganisms in heterotrophic biofilm from a deep-sea hydrothermal chimney. *Microb. Ecol.* <https://doi.org/10.1007/s00248-019-01381-z> (2019).
14. Marshall, C. W., Ross, D. E., Fichot, E. B., Norman, R. S. & May, H. D. Electrosynthesis of commodity chemicals by an autotrophic microbial community. *Appl. Environ. Microbiol.* **78**, 8412–8420 (2012).
15. Marshall, C. W., Ross, D. E., Fichot, E. B., Norman, R. S. & May, H. D. Long-term operation of microbial electrosynthesis systems improves acetate production by autotrophic microbiomes. *Environ. Sci. Technol.* **47**, 6023–6029 (2013).
16. Lim, J. K., Jung, H.-C., Kang, S. G. & Lee, H. S. Redox regulation of SurR by protein disulfide oxidoreductase in *Thermococcus onnurineus* NA1. *Extremophiles* <https://doi.org/10.1007/s00792-017-0919-1> (2017).
17. McCully, A. L. & Spormann, A. M. Direct cathodic electron uptake coupled to sulfate reduction by *Desulfovibrio ferrophilus* IS5 biofilms. *Environ. Microbiol.* **22**, 4794–4807 (2020).
18. Vorholt, J. A., Hafenbradl, D., Stetter, K. O. & Thauer, R. K. Pathways of autotrophic CO<sub>2</sub> fixation and of dissimilatory nitrate reduction to N<sub>2</sub>O in *Ferroglobus placidus*. *Arch. Microbiol.* **167**, 19–23 (1997).
19. Brileya, K. & Reysenbach, A.-L. The Class *Archaeoglobi*. In *The Prokaryotes* 15–23 (Springer, 2014). [https://doi.org/10.1007/978-3-642-38954-2\\_323](https://doi.org/10.1007/978-3-642-38954-2_323).
20. Amin Ali, O. *et al.* Iron corrosion induced by the hyperthermophilic sulfate-reducing archaeon *Archaeoglobus fulgidus* at 70 °C. *Int. Biodeterior. Biodegrad.* **154**, 105056 (2020).



21. Pillot, G. *et al.* Thriving of hyperthermophilic microbial communities from a deep-sea sulfidic hydrothermal chimney under electrolithoautotrophic conditions with nitrate as electron acceptor. *bioRxiv* <https://doi.org/10.1101/2021.03.26.437165> (2021).
22. Fuchs, G. Alternative pathways of carbon dioxide fixation: Insights into the early evolution of life?. *Annu. Rev. Microbiol.* **65**, 631–658 (2011).
23. Hamilton, W. A. Biofilms: Microbial interactions and metabolic activities. In *Ecology of Microbial Communities* (eds. Fletcher, M., Gray, T. R. G. & Jones J. G.) 361–385 (Cambridge University Press, 1987).
24. Kato, S., Hashimoto, K. & Watanabe, K. Microbial interspecies electron transfer via electric currents through conductive minerals. *Proc. Natl. Acad. Sci.* **109**, 10042–10046 (2012).
25. Lovley, D. R. Syntrophy goes electric: Direct interspecies electron transfer. *Annu. Rev. Microbiol.* **71**, 643–664 (2017).
26. Fast, A. G. & Papoutsakis, E. T. Stoichiometric and energetic analyses of non-photosynthetic CO<sub>2</sub>-fixation pathways to support synthetic biology strategies for production of fuels and chemicals. *Curr. Opin. Chem. Eng.* **1**, 380–395 (2012).
27. Berg, I. A. *et al.* Autotrophic carbon fixation in archaea. *Nat. Rev. Microbiol.* **8**, 447–460 (2010).
28. Yamamoto, M. *et al.* Spontaneous and widespread electricity generation in natural deep-sea hydrothermal fields. *Angew. Chem. Int. Ed.* **56**, 5725–5728 (2017).
29. Björkqvist, S., Ansell, R., Adler, L. & Lidén, G. Physiological response to anaerobicity of glycerol-3-phosphate dehydrogenase mutants of *Saccharomyces cerevisiae*. *Appl. Environ. Microbiol.* **63**, 128–132 (1997).
30. Furdul, C. & Ragsdale, S. W. The role of pyruvate ferredoxin oxidoreductase in pyruvate synthesis during autotrophic growth by the Wood-Ljungdahl pathway. *J. Biol. Chem.* **275**, 28494–28499 (2000).
31. Corre, E., Reysenbach, A.-L. & Prieur, D. *e*-Proteobacterial diversity from a deep-sea hydrothermal vent on the Mid-Atlantic Ridge. *FEMS Microbiol. Lett.* **205**, 329–335 (2001).
32. Jaeschke, A. *et al.* Microbial diversity of Loki's Castle black smokers at the Arctic Mid-Ocean Ridge. *Geobiology* **10**, 548–561 (2012).
33. Reysenbach, A.-L., Longnecker, K. & Kirshtein, J. Novel bacterial and archaeal lineages from an in situ growth chamber deployed at a Mid-Atlantic Ridge hydrothermal vent. *Appl. Environ. Microbiol.* **66**, 3798–3806 (2000).
34. Schrenk, M. O., Kelley, D. S., Delaney, J. R. & Baross, J. A. Incidence and diversity of microorganisms within the walls of an active deep-sea sulfide chimney. *Appl. Environ. Microbiol.* **69**, 3580–3592 (2003).
35. Schrenk, M. O., Brazelton, W. J. & Lang, S. Q. Serpentinization, carbon, and deep life. *Rev. Mineral. Geochem.* **75**, 575–606 (2013).
36. Lin, T. J. *et al.* Linkages between mineralogy, fluid chemistry, and microbial communities within hydrothermal chimneys from the Endeavour Segment, Juan de Fuca Ridge. *Geochim. Geophys. Geosyst.* **17**, 300–323 (2016).
37. Wirth, R. Colonization of black smokers by hyperthermophilic microorganisms. *Trends Microbiol.* **25**, 92–99 (2017).
38. Albuquerque, L. & Costa, M. S. da. The Family *Thermaceae*. In *The Prokaryotes* 955–987 (Springer, 2014). [https://doi.org/10.1007/978-3-642-38954-2\\_128](https://doi.org/10.1007/978-3-642-38954-2_128).
39. Lyons, C. M., Justin, P., Colby, J. & Williams, E. Isolation, characterization and autotrophic metabolism of a moderately thermophilic carboxydobacterium, *Pseudomonas thermocarboxydovorans* sp. nov.. *Microbiology* **130**, 1097–1105 (1984).
40. Palleroni, N. J. *Pseudomonas*. In *Bergey's Manual of Systematics of Archaea and Bacteria* 1–1 (American Cancer Society, 2015). <https://doi.org/10.1002/9781118960608.gbm01210>.
41. Droffner, M. L., Brinton, W. F. & Evans, E. Evidence for the prominence of well characterized mesophilic bacteria in thermophilic (50–70°C) composting environments. *Biomass Bioenergy* **8**, 191–195 (1995).
42. Shen, H.-B. *et al.* Enhanced bioelectricity generation by improving pyocyanin production and membrane permeability through sophorolipid addition in *Pseudomonas aeruginosa*-inoculated microbial fuel cells. *Bioresour. Technol.* **167**, 490–494 (2014).
43. Maruthupandy, M., Anand, M., Maduraiveeran, G., Beevi, A. S. H. & Priya, R. J. Electrical conductivity measurements of bacterial nanowires from *Pseudomonas aeruginosa*. *Adv. Nat. Sci. Nanosci. Nanotechnol.* **6**, 045007 (2015).
44. Lai, B. *et al.* Anoxic metabolism and biochemical production in *Pseudomonas putida* F1 driven by a bioelectrochemical system. *Biotechnol. Biofuels* **9**, 39 (2016).
45. Reimers, C. E. *et al.* Microbial fuel cell energy from an ocean cold seep. *Geobiology* **4**, 123–136 (2006).
46. Vos, P. D. Bacillales. In *Bergey's Manual of Systematics of Archaea and Bacteria* 1–1 (American Cancer Society, 2015). <https://doi.org/10.1002/9781118960608.obm00057>.
47. Dahle, H. *et al.* Energy landscapes in hydrothermal chimneys shape distributions of primary producers. *Front. Microbiol.* **9**, 1570 (2018).
48. Sarradin, P.-M. & Cannat, M. MOMARSAT2014 cruise, Pourquoi pas ?. *R/V.* <https://doi.org/10.17600/14000300> (2014).
49. Schleucher, J. *et al.* A general enhancement scheme in heteronuclear multidimensional NMR employing pulsed field gradients. *J. Biomol. NMR* **4**, 301–306 (1994).
50. Zhang, L. *et al.* Bacterial and archaeal communities in the deep-sea sediments of inactive hydrothermal vents in the Southwest India Ridge. *Sci. Rep.* **6**, 1–11 (2016).
51. Bates, S. T. *et al.* Examining the global distribution of dominant archaeal populations in soil. *ISME J.* **5**, 908–917 (2011).
52. Kumar, S., Stecher, G., Li, M., Knyaz, C. & Tamura, K. MEGA X: Molecular evolutionary genetics analysis across computing platforms. *Mol. Biol. Evol.* **35**, 1547–1549 (2018).

## Acknowledgements

This work received financial support from the CNRS-sponsored national interdisciplinary research program (PEPS-ExoMod 2016). The authors thank Céline Rommevaux and Françoise Lesongeur for taking samples during the MOMARSAT 2014 cruise, the MIM platform (MIO, France) for providing access to their confocal microscopy facility, and the GeT-PlaGe platform (GenoToul, France) for help with DNA sequencing. The project leading to this publication received European FEDER funding under Project No. 1166-39417. The authors declare no conflicts of interest.

## Author contributions

G.P. and P.P.L. designed research with assistance from S.D. and Y.C.B.; G.P., S.D. and P.P.L. performed research; G.P., S.D., A.G., Y.C.B. and P.P.L. analyzed data; L.S. developed and implemented the NMR analyses; and G.P. and P.P.L. wrote the paper with assistance from O.A.A. and P.B.

## Competing interests

The authors declare no competing interests.

## Additional information

**Supplementary Information** The online version contains supplementary material available at <https://doi.org/10.1038/s41598-021-94135-2>.

**Correspondence** and requests for materials should be addressed to P.-P.L.

**Reprints and permissions information** is available at [www.nature.com/reprints](http://www.nature.com/reprints).

**Publisher's note** Springer Nature remains neutral with regard to jurisdictional claims in published maps and institutional affiliations.



**Open Access** This article is licensed under a Creative Commons Attribution 4.0 International License, which permits use, sharing, adaptation, distribution and reproduction in any medium or format, as long as you give appropriate credit to the original author(s) and the source, provide a link to the Creative Commons licence, and indicate if changes were made. The images or other third party material in this article are included in the article's Creative Commons licence, unless indicated otherwise in a credit line to the material. If material is not included in the article's Creative Commons licence and your intended use is not permitted by statutory regulation or exceeds the permitted use, you will need to obtain permission directly from the copyright holder. To view a copy of this licence, visit <http://creativecommons.org/licenses/by/4.0/>.

© The Author(s) 2021